

Improved Adaptive Type-2 Fuzzy Filter with Exclusively Two Fuzzy Membership Function for Filtering Salt and Pepper Noise

Vikas Singh, *Student Member, IEEE*, Pooja Agrawal, Teena Sharma, *Student Member, IEEE*, and Nishchal K Verma, *Senior Member, IEEE*

Abstract—Image denoising is one of the preliminary steps in image processing methods in which the presence of noise can deteriorate the image quality. To overcome this limitation, in this paper a improved two-stage fuzzy filter is proposed for filtering salt and pepper noise from the images. In the first-stage, the pixels in the image are categorized as good or noisy based on adaptive thresholding using type-2 fuzzy logic with exclusively two different membership functions in the filter window. In the second-stage, the noisy pixels are denoised using modified ordinary fuzzy logic in the respective filter window. The proposed filter is validated on standard images with various noise levels. The proposed filter removes the noise and preserves useful image characteristics, i.e., edges and corners at higher noise level. The performance of the proposed filter is compared with the various state-of-the-art methods in terms of peak signal-to-noise ratio and computation time. To show the effectiveness of filter statistical tests, i.e., Friedman test and Bonferroni–Dunn (BD) test are also carried out which clearly ascertain that the proposed filter outperforms in comparison of various filtering approaches.

Index Terms—Salt and pepper noise, fuzzy set, PSNR, structural similarity index, statistical test, type-2 fuzzy set.

LIST OF ABBREVIATIONS

SAP	Salt and Pepper
MF	Membership Function
PSNR	Peak Signal-to-Noise Ratio
LMF	Lower Membership Function
UMF	Upper Membership Function
BD	Bonferroni-Dunn
CD	Critical Difference

I. INTRODUCTION

IMAGES gets corrupted with Salt and Pepper (SAP) noise during image acquisition, coding, transmission and processing through various sensors or communication channels. The SAP noise is randomly distributed in the form of black and white pixels in the digital images. It is essential, and even highly desirable to remove it from the images to expedite the subsequent image processing operations, such as image segmentation, edge detection, object recognition, etc.

In the literature, various filtering techniques have been proposed to filter out the SAP noise from images. Non-linear filtering techniques generally performed better in comparison

of linear filtering techniques, because, these filters use the ranking information of pixels in the filter window. The non-linear filtering techniques, i.e. standard median (SM) filter was initially proposed for filtering the SAP noise from the images [1], [2]. But, the problem with the SM filter is that it does not preserve relevant image details at higher noise level. To overcome the limitations of SM filter, various approaches have been proposed such as weighted median (WM) filter [3] and center weighted median (CWM) filter [4]. In WM filter, the filtering performance is controlled by a set of weighting parameters, whereas in CWM filter, only central pixel is weighted in the filter window. Zhang *et al.* [5] proposed a new adaptive weighted mean filter based on window size enlarging for detecting and denoising the high level of SAP noise. Again, these filters also have certain limitation in weight assignment. To address such issue, Chen *et al.* [6] presented a weighted couple sparse representation model between reconstructed and noisy image to remove the impulse noise. Liu *et al.* [7] have presented as space coding based method for mixed noise removal. In [8], soft thresholding method is proposed to nullify the effect of small weights at image edges. A multi-class support vector machine based adaptive filter is also proposed for the removal of SAP noise from images [9]. But the problem with these filters is that they do not preserve the desired image characteristics, i.e., edges and corners at higher noise level.

In the past, fuzzy filters were more popular due to their simplicity and efficiency, especially when adaptive setting is required. The weighted fuzzy mean (WFM) [10], adaptive fuzzy (AF) [11], iterative adaptive fuzzy (IAF) [12] and adaptive fuzzy switching weighted mean [13] filters were proposed to remove SAP noise. In WFM filter, the output is replaced by membership value with their associated fuzzy rule base, whereas AF filter uses the adaptive window enlarging to detect and denoise the impulse noise from the images. These filters also have weight assignment problem in the filter window. The IAF is a two-stage filter with the first-stage is for detection of noisy pixel by fuzzy threshold which is heuristic in nature and second-stage is for denoising of detected noisy pixel. Adaptive fuzzy filter based on the fuzzy transform is also presented for removal of impulse noise from images [14], [15]. Wang *et al.* [16] have also proposed two-stage filter based on adaptive fuzzy switching for SAP noise removal. In [17], fuzzy mathematical morphology open-close filter is presented for filtering the impulse noise. Roy *et al.* [18] have presented region adaptive fuzzy filter for removal of random-

Vikas Singh, Pooja Agrawal, Teena Sharma & Nishchal K Verma are with the Dept. of Electrical Engineering, Indian Institute of Technology Kanpur, India (e-mail: vikkyk@iitk.ac.in, pooja.iitd@gmail.com, teenashr@iitk.ac.in, nishchal.iitk@gmail.com)

valued impulse noise. But the common problem with ordinary fuzzy set is that they are not sufficient to model the uncertainty in noisy environment because membership value assigned to pixels are themselves noisy [19].

To overcome the limitations of ordinary fuzzy set, a type-2 fuzzy set was proposed by Zadeh [20]. The type-2 fuzzy set has primary membership function and corresponding to each primary membership function there is a secondary membership function (MF) [21], [22]. Liang and Mendel have presented an adaptive fuzzy filter using type-2 Takagi-Sugeno-Kang (TSK) fuzzy model for equalization of non-linear time varying channels [23]. Yldrm *et al.* [24] have presented a details preserving filter using type-2 fuzzy set and validated the performance on various noise densities. In [25], Khanesar *et al.* have presented a fuzzy filter based on type-2 fuzzy MF for noise reduction from noisy environment. Yuksel and Basturk have presented a fuzzy filter based on type-2 fuzzy for filtering salt and pepper noise from images [26]. Zhai *et al.* [27] have proposed a fuzzy filter for filtering the mixed Gaussian and impulse noise using interval type-2 fuzzy model. But the problem among these approaches is formation of a large rule base which increases the computational complexity of the filters.

To overcome the above limitations in this paper, a improved two-stage fuzzy filter is proposed for detection and denoising of noisy pixels from images. In the first-stage, noisy pixels are detected using an adaptive threshold by type-2 fuzzy logic. The proposed threshold is decided by only two primary MFs which eliminate the problem of $\frac{N+1}{2}$ number of primary MFs in approach [28] (N be the number of pixels in a filter window). The proposed threshold is very effective and efficient in comparison of state-of-the-art. In the second-stage, pixels in the image are categorized as noisy in first-stage is denoised. For denoising of detected noisy pixels, good pixels are used in their respective filter window. To assign appropriate weight to good pixels a modified fuzzy logic based method is also presented. The proposed two-stage fuzzy filter preserves desired image characteristics such as edges and corners at higher noise level. The proposed filter is validated on standard datasets [40] with different noise levels. The result shows that the proposed filter performs quantitatively and qualitatively better in comparison to various state-of-the-art methods.

The rest of the paper is organized as: Preliminaries of proposed schemes are described in Section II. Proposed adaptive type-2 fuzzy threshold and modified denoising approach are described in Section III. Experimentation, discussion, and comparison with various state-of-the-art methods are presented in Section IV. Finally, Section V concludes the paper.

II. PRELIMINARIES

A. Ordinary fuzzy set

If I is a collection of attributes (pixels) in the image denoted by p_{ij} located at i^{th} row and j^{th} column, then a fuzzy set \mathbf{P}_{ij}^H in I is defined as

$$\mathbf{P}_{ij}^H = \left\{ (p_{ij}, \mu_{\mathbf{P}_{ij}^H}) \mid p_{ij} \in I \right\} \quad (1)$$

where $\mu_{\mathbf{P}_{ij}^H}$ is called MF as shown in Fig.1, which maps each element of I between 0 and 1 [29]–[35]. The superscript H in the MF represents filter window half-size parameter.

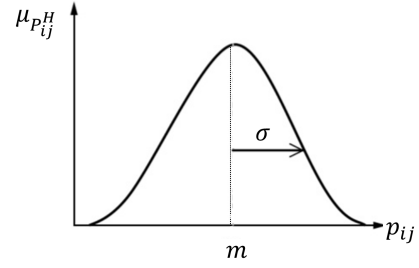


Figure 1: Type-1 fuzzy Gaussian MF [29].

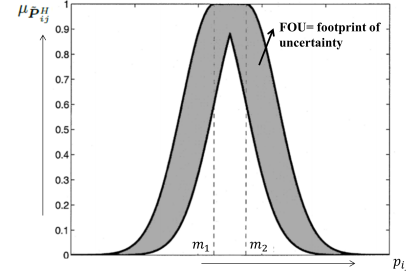


Figure 2: Interval type-2 fuzzy MF with different means [36].

B. Type-2 fuzzy set

A type-2 membership value can be any subset $\in [0, 1]$ in the primary membership, corresponding to each primary membership there is a secondary membership which also mapped in $[0, 1]$ [36]–[38]. An interval type-2 fuzzy set $\tilde{\mathbf{P}}_{ij}^H$ characterized by MF $\mu_{\tilde{\mathbf{P}}_{ij}^H}$ as shown in Fig. 2 is defined as

$$\tilde{\mathbf{P}}_{ij}^H = \left\{ \left((p_{ij}, \mu_{\mathbf{P}_{ij}^H}), \mu_{\tilde{\mathbf{P}}_{ij}^H}(p_{ij}, \mu_{\mathbf{P}_{ij}^H}) \right) \mid \forall p_{ij} \in I, \right. \\ \left. \forall \mu_{\mathbf{P}_{ij}^H} \in J_{p_{ij}} \subseteq [0, 1] \right\} \quad (2)$$

where $0 \leq \mu_{\mathbf{P}_{ij}^H}, \mu_{\tilde{\mathbf{P}}_{ij}^H}(p_{ij}, \mu_{\mathbf{P}_{ij}^H}) \leq 1$.

C. Neighborhood pixel set

A neighborhood pixel set \mathbf{P}_{ij}^H is the collection of pixel $p_{ij} \in I$ with half filter window of size H can be defined as

$$\mathbf{P}_{ij}^H = \left\{ p_{i+q, j+l}, \forall q, l \in [-H, H] \right\} \quad (3)$$

The neighborhood pixel \mathbf{P}_{ij}^H has N elements in the filter window. Here, the size of N is $(2H + 1)^2$.

III. PROPOSED SCHEMES

To filter out the SAP noise from digital images, an improved two-stage fuzzy filtering approach is described in this section. The first-stage of the filter describes the detection of pixels corrupted by SAP noise in the image followed by the second-stage, denoising of those corrupted pixels. For detection of corrupted pixels, adaptive type-2 fuzzy threshold is explained and an ordinary fuzzy logic based approach is also introduced for denoising of corrupted pixels. The schematic of the proposed filter is shown in Fig. 3 and explained in the following subsections.

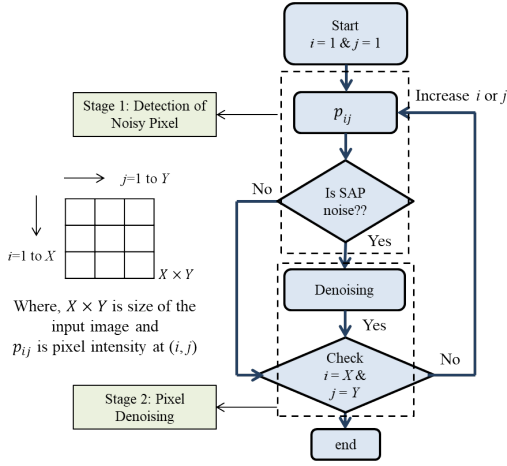


Figure 3: Flowchart for the proposed two-stage fuzzy filter.

A. First-Stage: Finding the Adaptive Threshold

Initially, the upper membership function (UMF) and lower membership function (LMF) of type-2 fuzzy set are designed for finding adaptive threshold to detect the noisy pixels in the filter window. In the previous literature's [12], [28], primary Gaussian MFs depend upon *mean of k-middle* (where, $k = 1, 2, \dots, \frac{N+1}{2}$ and N be the number of pixels in a filter window), e.g. at low noise, the size of H is 1 and for this filter window, UMF and LMF are decided by 5 different primary Gaussian MFs. But at higher noise level, H increases and large number of primary Gaussian MFs are drawn to find the UMF and LMF to decide the threshold, whereas in proposed approach primary Gaussian MFs are drawn by applying the classical mean on number of pixels in the filter window except the middle pixel to determined the *means* and the *variance* in the respective filter window. Herein, only two different *means* are determined for any size of filter window in order to draw the two different primary Gaussian MFs with same *variance*. These two primary Gaussian MFs are used to determine the UMF and LMF for finding the adaptive threshold to detect the noisy pixel within the respective filter window.

Initially, a filter window of size $(2H + 1) \times (2H + 1)$ is chosen in the image I for the calculation of neighborhood pixel set \mathbf{P}_{ij}^H . The pixel $p_{ij} \in \{0, 1\}$ is at the center of the filter window, initially the half filter window (H) is set to be 1 for simplicity. Then, an ordinary fuzzy set \mathbf{P}_{ij}^H is defined in the universe of discourse I for all N pixels in the respective filter window. The membership function $\mu_{\mathbf{P}_{ij}^H}(p_{ij}) : \mathbf{P}_{ij}^H \rightarrow [0, 1]$ is called as primary membership function. Then, the primary Gaussian MFs are designed using two different *means* (m_1^H and m_2^H) with same *variance* (σ^H) as shown in Fig. 4.

The membership values of each primary Gaussian MF are themselves a fuzzy set, which also map in the interval $[0, 1]$ called as secondary membership function as defined in (2) and shown in Fig. 5.

For every pixel p_{ij} in neighborhood pixel set \mathbf{P}_{ij}^H , a Gaussian membership function with *mean* (m_k^H , where, $k = 1, 2$) and *variance* (σ^H) is defined as

$$\mu_{\mathbf{P}_{ij}^H(k)}(p_{ij}) = \exp - \frac{1}{2} \left(\frac{p_{ij} - m_k^H}{\sigma^H} \right)^2 \quad (4)$$

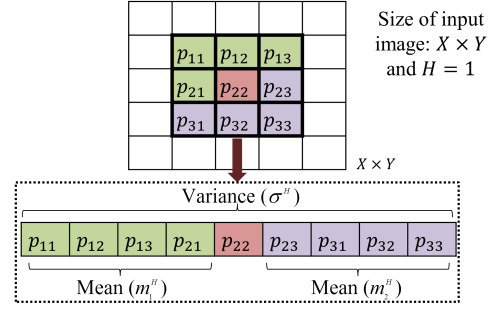


Figure 4: Mean and variance values of primary MFs in 3×3 window.

The Gaussian membership function parameters, i.e., *means* (m_k^H) are varied according to the values of k for all pixels in the filter windows as

$$m_k^H = \begin{cases} \frac{2}{N-1} \sum_{r=1}^h p_r, & \forall p_r \in \mathbf{P}_{ij}^H, \& k = 1 \\ \frac{2}{N-1} \sum_{r=h+2}^N p_r, & \forall p_r \in \mathbf{P}_{ij}^H, \& k = 2 \end{cases} \quad (5)$$

where $h = \frac{N-1}{2}$, $p_r = p_{ij}$ be the pixel intensity at location (i, j) in the filter window.

The *variance* (σ^H) is found using all the pixels in respective filter windows as

$$\sigma^H = \frac{1}{N} \sum_{q,l} \omega_{i+q,j+l}^H, \quad \forall q, l \in [-H, H] \quad (6)$$

The parameter $\omega_{i+q,j+l}^H$ is calculated using l_1 norm.

$$\omega_{i+q,j+l}^H = s |p_{i+q,j+l} - \nu_{avg}|, \quad \forall q, l \in [-H, H] \quad (7)$$

where $s > 1$ is the scaling factor and

$$\nu_{avg} = \frac{1}{2} \sum_{k=1}^2 m_k^H \quad (8)$$

Using (4)-(6), the upper ($\bar{\mu}(p_r)$) and lower ($\underline{\mu}(p_r)$) membership functions in a filter window are written as

$$\bar{\mu}(p_r) = \begin{cases} \mu_{\mathbf{P}_{ij}^H(1)}(m_1^H, \sigma^H), & \text{if } p_r^H < m_1^H \\ \vee (\mu_{\mathbf{P}_{ij}^H(1)}(p_r), \mu_{\mathbf{P}_{ij}^H(2)}(p_r)), & \text{if } m_1^H \leq p_r^H \leq m_2^H \\ \mu_{\mathbf{P}_{ij}^H(2)}(m_2^H, \sigma^H), & \text{if } p_r^H > m_2^H \end{cases} \quad (9)$$

$$\underline{\mu}(p_r) = \begin{cases} \mu_{\mathbf{P}_{ij}^H(2)}(m_2^H, \sigma^H), & \text{if } p_r^H \leq \frac{m_1^H + m_2^H}{2} \\ \mu_{\mathbf{P}_{ij}^H(1)}(m_1^H, \sigma^H), & \text{if } p_r^H > \frac{m_1^H + m_2^H}{2} \end{cases}$$

As shown in Fig. 4, two different *means* and *variance* of primary Gaussian MFs are calculated using (5) and (6) in respective filter window. The plot for two primary MFs with their UMF and LMF are shown in Fig. 5.

Let us define a matrix $\tilde{\mu}$ consisting membership values of both upper and lower MFs in the filter window. Basically, $\tilde{\mu}$ has two different membership values corresponding to each pixels in the filter window and written as

$$\tilde{\mu} = \begin{bmatrix} \bar{\mu}(p_r) \\ \underline{\mu}(p_r) \end{bmatrix} \quad (10)$$

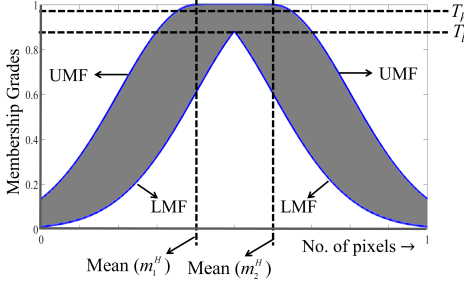


Figure 5: Adaptive threshold using type-2 fuzzy MF.

where $\bar{\mu}(p_r)$ and $\underline{\mu}(p_r)$ are the row vectors consisting upper and lower membership values from $r = 1, 2, \dots, N$ in the filter window.

A column and row-wise S-norm (max-operation) and a column-wise T-norm (min-operation) followed by S-norm operation is performed on the matrix $\tilde{\mu}$ to obtain the upper and lower threshold T_h and T_l as shown in Fig. 5 and given in (11). In proposed approach, T_h represents the deciding threshold for categorizing a pixel as good or noisy in the filter window and T_l be the maximum value of the LMF in the same window and they can be defined as

$$T_h = \vee(\vee(\tilde{\mu})); \quad T_l = \vee(\wedge(\tilde{\mu})) \quad \forall q, l \in [-H, H] \quad (11)$$

where \wedge and \vee are the minimum and maximum operators, respectively.

The threshold T_h is adaptive and varies according to the SAP noise level in the filter window. In matrix $\tilde{\mu}$, two different MFs are associated with every pixel in the filter window. A set of membership values $\mu_{P_{ij}^H}$ associated with neighborhood pixel vector P_{ij}^H is the column-wise average value of the matrix $\tilde{\mu}$ and expressed as

$$\Delta\mu_{P_{ij}^H} = \frac{1}{2}(\bar{\mu}(p_r) + \underline{\mu}(p_r)) \quad (12)$$

Finally, the membership value $\Delta\mu_{P_{ij}^H}$ of every single pixel in a filter window is obtained and compared with the threshold T_h in the respective filter window. If the membership value $\Delta\mu_{P_{ij}^H}$ is greater than or equal to T_h , then it is considered as a good pixel else noisy pixel as given in (13). If the center pixel in the filter window has membership value greater than or equal to T_h , then it is assumed to be good pixel.

$$p_r = \begin{cases} \text{good pixel,} & \text{if } \Delta\mu_{P_{ij}^H}(r) \geq T_h \\ \text{noisy pixel,} & \text{if } \Delta\mu_{P_{ij}^H}(r) < T_h \end{cases} \quad (13)$$

where $r = 1, 2, \dots, N$ and $T_l < T_h \leq 1$.

The value of the threshold T_h become 1 when there is uniform pixel intensity distribution in the filter window.

B. Second-Stage: Denoising using Ordinary Fuzzy Logic

In this stage, pixels categorized as noisy in first-stage are denoised in the respective filter window. The number of good pixels in the respective filter window plays an important role for denoising the detected noisy pixels. Therefore, selection of relevant weights for these good pixels are essential. The denoising methods present in the literature's are mostly inverse

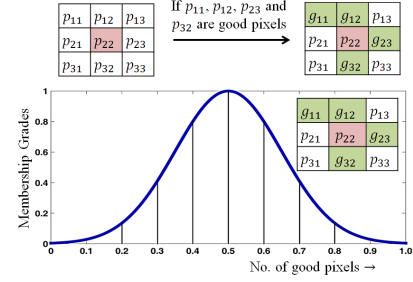


Figure 6: Type-1 MF for denoising noisy pixels in 3×3 window.

weighting distance based or ordinary fuzzy set, i.e., type-1 fuzzy set based. The drawback of inverse distance based methods are the assignment of weight to good pixels in the filter window, whereas in type-1 fuzzy set based methods the appropriate weights corresponding to each good pixels are determined using Gaussian MF. The *mean* and *variance* of the MF is determined using *mean of k-middle* in a filter window which increases the computational complexity of the filter.

To overcome the above problems in this denoising approach, a classical mean has been used to determine the *mean* of the Gaussian MF. For this purpose, set of good pixels G are considered in respective filter window. These good pixels are considered as fuzzy set and they are mapped in interval $[0, 1]$ with MF μ_G . Applying this approach on every good pixel in the filter window have different membership value and they act as weighting parameter corresponding to each good pixels. Firstly, *mean* of Gaussian MF is computed using all good pixels in the filter window of size $(2H + 1) \times (2H + 1)$ and *variance* is computed using l_1 norm of the good pixels with respect to *mean* in the same filter window as given in (14) and (15). The Gaussian MF plots corresponding to good pixels in a 3×3 window (where, g_{11} , g_{12} , g_{23} and g_{32} are the good pixels) is shown in Fig. 6.

The *mean* (m) and *variance* (σ_G) values of good pixels for Gaussian MF (μ_G) in a filter window are determined as

$$m = \frac{1}{\rho} \sum_{i=1}^{\rho} g_i; \quad \sigma_G = \frac{1}{\rho} \sum_{i=1}^{\rho} \omega_i \quad (14)$$

where ρ be the number of good pixels in the filter window and g_i be the i^{th} ($i = 1, 2, \dots, \rho$) good pixels in fuzzy set G . The parameter ω_i is calculated using l_1 norm as

$$\omega_i = s|G - m| \quad \forall i \in G \quad (15)$$

The Gaussian MF (μ_G) corresponding to the good pixels is calculated as

$$\mu_G(g_i) = \exp -\frac{1}{2} \left(\frac{g_i - m}{\sigma_G} \right)^2 \quad (16)$$

Finally, the denoised pixel intensity p^{new} corresponding to noisy pixels are determined as

$$p^{\text{new}} = \frac{\sum_{\forall g_i \in G} w_i g_i}{W}; \quad W = \sum_{i=1}^{\rho} w_i \quad (17)$$

where $w_i \in \mu_G$ be the weight corresponding to the i^{th} good pixel in the filter window and W be the normalizing parameter.

In case of higher noise level, there is a chance that the number of good pixels in filter window will become zero. In such cases, the parameter H is increased by 1 and the complete step (first stage and second stage as described in subsections III-A and III-B) is repeated. If σ_G is below with a small threshold ϵ or near to zero due to uniform pixel intensities distribution, then the pixel p_{ij} is simply replaced by their mean (m) and this will limit the division by zero in (16). The complete procedures of the proposed filter is illustrated in Algorithm 1.

Algorithm 1 Noise removal using proposed schemes

```

1: for every pixels  $p_r \in I$  do
2:   if  $p_r \notin \{0, 1\}$  then
3:     retain  $p_r$ ;
4:     continue
5:   while  $p_r \in \{0, 1\}$  do
6:     initialize  $H = 1$ 
7:     Compute  $P_{ij}^H$  using (3) and  $\Delta\mu_{P_{ij}^H}$  using (12)
8:     if  $\Delta\mu_{P_{ij}^H}(p_r) \geq T_h$  then
9:       retain  $p_r$ 
10:      break
11:    if  $\sigma^H \leq \epsilon$  then
12:       $p_r = m$ ;
13:      break
14:    Compute  $G_{ij}^H$  using (13)
15:     $\rho = |G_{ij}^H|$ 
16:    if  $\rho < 1$  then
17:       $H = H + 1$ 
18:    continue
19:    Compute  $p^{new}$  using (14) – (17)
20:    break
21:  end while
22: end for

```

IV. EXPERIMENTAL RESULTS & VALIDATION

The proposed two-stage fuzzy filter has been validated on five standard gray scale images [40], i.e. Baboon, Barbara, Boat, Lena and Peppers of resolution 512×512 . The performance of the proposed filter is measured quantitatively by PSNR and for qualitative analysis, performance of the proposed filter is validated at different noise level. In addition to show the effectiveness of proposed filter statistical test is also provided in next subsections.

In the proposed filter, the variable parameter k takes only two different values, i.e., 1 and 2 to compute two different means with same variance of primary Gaussian membership functions as given in (5) and (6) to decide the upper and lower MFs in the filter window as given by (9). The upper and lower membership values corresponding to all pixels in the filter window are stored in the matrix $\tilde{\mu}$ where, $\bar{\mu}(p_r)$ and $\underline{\mu}(p_r)$ are the row vectors consisting upper and lower membership values from $r = 1, 2, \dots, N$ in the filter window. A column and row-wise max-operation applied on the $\tilde{\mu}$ to obtain the threshold

values T_h . The obtained threshold is adaptive and varied according to salt and pepper noise level. If the membership values corresponding to the pixel in the filter window is greater than or equal to T_h then this pixel in the filter is treated as good pixel otherwise noisy pixel. If the detected pixel is treated as noisy in the filter window then a set of good pixel is chosen to denoise the noisy pixel as described in section III-B. After applying the noise detection and denoising approaches as described in Algorithm 1 the Table I shows that the PSNR values of proposed approach is better in comparison of several state-of-the-art methods namely, adaptive type-2 fuzzy filter (AT2FF) [28], Iterative adaptive fuzzy filter (IAF) [13], fast median (FM) [41], contrast enhancement based filter (CEF) [42], pixel-wise S-estimate (PWS) [43], adaptive median with edge-preserving regularization (AMEPR) [44], different applied median filter (DAMF) [48], boundary discriminative noise detection (BDND) [45], cloud model (CM) filter [46] and spatially adaptive total variation filter (SATV) [47]. In case of Baboon the PSNR at low noise level is comparative to IAF but it is better for higher noise level.

The PSNR is defined using filtered image (I_f) with respect to actual image (I_o) as

$$PSNR(I_o, I_f) = 10 \log_{10} \frac{(255)^2}{\frac{1}{XY} \sum_{i,j} (I_o(i,j) - I_f(i,j))^2} \quad (18)$$

where 255 be the highest pixel intensity value of 8 bit grayscale image.

For quantitative analysis, the performance in terms of PSNR values with three different noise level, i.e., 20%, 50%, and 80% are provided in Table I. At noise level 50% and 80%, filtered images of Baboon and Barbara are shown in Figs. 7c, 7e, 8c and 8e, respectively. For noise level of 97% and 99%, filtered images of Lena and Peppers are shown in Fig. 9c and 9f. As shown in Fig. 9f, the proposed filter also preserves useful image details even at 99% noise level.

For experimentation, minimum number of good pixels (ρ_{min}) is set to 1 in filter window to find the correct pixel value of noisy pixels. This is because a large number of good pixels are needed for denoising of noisy pixel in the respective filter window. For generalization purpose the whole experimentation is run for ten iteration independently and average value of the PSNR and average run time are computed as given in Table I and Table IV.

The average performance in terms of PSNR values at noise levels 20%, 50% and 80% are also provided in Figs. 10, 11 and 12, which shows that the noise filtering performance of the proposed approach is better in comparison of various state-of-the-art methods.

A. Statistical Test of Quantitative Measures

The performance analysis of the proposed algorithm is further evaluated using statistical analysis for the quantitative measures. The statistical evaluation of experimental results has been considered an essential part for the generalization of methods. In this subsection, we have performed two statistical test, i.e., Friedman test and Bonferroni–Dunn (BD)

Table I: COMPARISON OF PERFORMANCE WITH VARIOUS STATE-OF-THE-ART METHODS (IN TERM OF PSNR (IN DB))

Dataset [40]	Noise (in %)	FM [41]	CEF [42]	PWS [43]	AMEPR [44]	BDND [45]	CM [46]	SATV [47]	IAF [12]	DAMF [48]	AT2FF [28]		Proposed Approach
											DMSV	DMDV	
Lena	20	37.05	37.46	36.85	38.21	38.52	39.42	39.20	39.92	39.12	40.75	40.79	41.07
	50	29.81	30.71	29.57	33.46	32.74	33.57	33.88	34.10	33.14	34.88	34.90	34.99
	80	23.11	23.22	22.68	27.16	27.11	28.45	27.14	28.84	28.47	28.92	28.89	29.24
Peppers	20	36.21	35.03	35.46	37.45	34.44	37.54	36.87	37.99	36.03	41.00	41.01	41.16
	50	29.53	30.38	29.26	31.25	30.23	32.03	31.62	32.34	29.35	35.17	35.14	35.31
	80	22.21	23.65	22.84	27.32	26.61	27.46	26.42	27.54	24.52	29.22	29.26	29.67
Baboon	20	27.22	26.85	26.82	29.87	27.73	28.47	28.49	29.75	28.96	29.30	29.29	29.38
	50	22.26	21.93	20.42	24.52	23.46	24.05	23.91	24.84	24.14	24.59	24.60	24.65
	80	18.69	17.60	17.86	19.73	19.92	20.36	20.59	20.73	20.65	20.79	20.81	20.85
Barbara	20	29.46	29.58	28.72	29.72	29.85	30.78	30.70	31.95	33.00	33.22	33.20	33.28
	50	23.46	23.37	22.69	25.33	25.17	26.10	25.91	26.74	27.72	28.24	28.26	28.28
	80	19.35	19.31	18.91	21.41	21.74	22.54	22.66	22.78	23.82	23.82	23.81	23.93
Boat	20	34.75	30.87	33.78	34.89	34.83	35.31	35.97	36.03	36.80	36.67	36.62	36.83
	50	27.96	25.65	26.80	29.34	29.68	29.99	30.38	30.69	30.86	31.39	31.38	31.41
	80	23.65	21.46	22.50	24.75	24.93	25.58	25.18	25.88	26.27	26.23	26.26	26.42

The values in bold represent better PSNR, *DMSV: Different mean same variance & **DMDV: different mean different variance

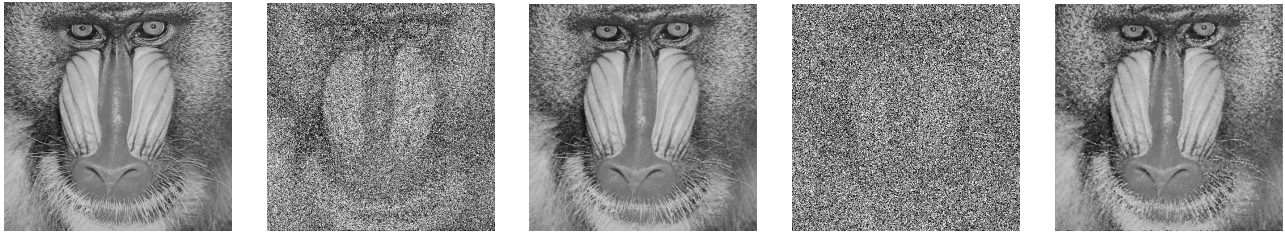


Figure 7: Baboon Image (a) Original Image (b) With 50% noise (c) Filtered image with 50% noise (d) With 80% noise (e) Filtered image with 80% noise.



Figure 8: Barbara Image (a) Original Image (b) With 50% noise (c) Filtered image with 50% noise (d) With 80% noise (e) Filtered image with 80% noise.



Figure 9: Filtered images at higher noise level (a) Lena - Original Image (b) Lena - With 97% noise (c) Lena - Filtered image with 97% noise (d) Peppers - Original Image (e) Peppers - With 99% noise (f) Peppers - Filtered image with 99% noise.

Table II: RANK OF THE PROPOSED APPROACH WITH VARIOUS STATE-OF-THE-ART METHODS

Dataset [40]	Noise (in %)	FM [41]	CEF [42]	PWS [43]	AMEPR [44]	BDND [45]	CM [46]	SATV [47]	IAF [12]	DAMF [48]	Proposed Approach
Lena	20	9	8	10	7	6	3	4	2	5	1
	50	9	8	10	6	7	4	3	2	5	1
	80	9	8	10	5	7	4	6	2	3	1
Pepper	20	6	9	8	4	10	3	5	2	7	1
	50	8	6	10	5	7	3	4	2	9	1
	80	10	8	9	4	5	3	6	2	7	1
Baboon	20	8	9	10	1	7	6	5	2	4	3
	50	8	9	10	4	7	5	6	1	3	2
	80	8	10	9	7	6	5	4	2	3	1
Barbara	20	10	8	9	7	6	4	5	3	2	1
	50	8	9	10	6	7	4	5	3	2	1
	80	8	9	10	7	6	5	4	3	2	1
Boat	20	8	10	9	6	7	5	4	3	2	1
	50	8	10	9	7	6	5	4	3	2	1
	80	8	10	9	7	6	4	5	3	2	1
Sum of ranks		125	131	142	83	100	63	70	35	60	18
Average rank		8.33	8.73	9.47	5.53	6.67	4.20	4.67	2.33	4.00	1.20

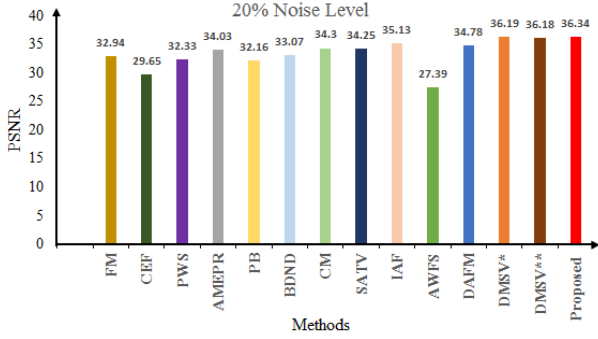


Figure 10: Mean PSNR at 20% level with different methods.

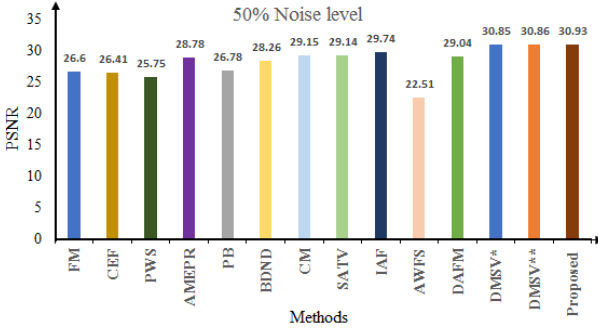


Figure 11: Mean PSNR at 50% level with different methods.

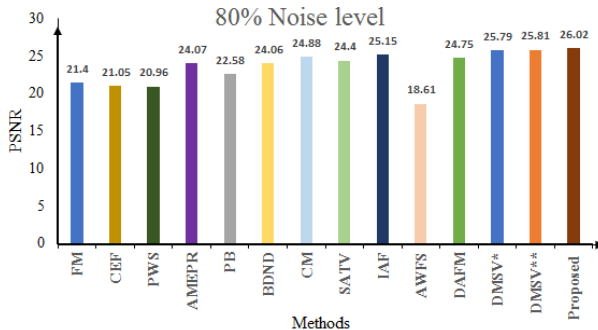


Figure 12: Mean PSNR at 80% level with different methods.

Table III: RANK OF THE PROPOSED APPROACH WITH AT2FF

Dataset [40]	SAP Noise (in %)	AT2FF [28]		Proposed Approach
		DMSV	DMDV	
Lena	20	3	2	1
	50	3	2	1
	80	2	3	1
Peppers	20	3	2	1
	50	2	3	1
	80	3	2	1
Baboon	20	2	3	1
	50	3	2	1
	80	3	2	1
Barbara	20	2	3	1
	50	3	2	1
	80	2	3	1
Boat	20	2	3	1
	50	2	3	1
	80	3	2	1
Sum of ranks		38	37	15
Average rank		2.53	2.47	1.00

test to examine the statistical significance of the results. The Friedman statistic is defined as

$$\chi^2 = \frac{12M}{l(l+1)} \left[\sum_{z=1}^l R_z^2 - \frac{l(l+1)^2}{4} \right] \quad (19)$$

$$F_F = \frac{(M-1)\chi^2}{M(l-1) - \chi^2} \quad (20)$$

where M be the number of datasets, l be the number of algorithms and R_z be the average rank of algorithm z among all datasets. The parameter F_F follows a Fisher distribution with $l-1$ and $(l-1) \times (M-1)$ degrees of freedom. The critical values of parameters χ^2 and F_F are found in Table A4 and Table A10 in [49].

If the calculated statistic using (23) and (24) is greater than the critical value then the Null Hypothesis is rejected. If the null hypothesis is rejected under the Friedman test, a posthoc test such as BD test is performed to determine which algorithms are statistically different than another. According to BD test, an algorithm is considered statistically better, if the difference of average rank between the algorithms are greater

Table IV: COMPARISON OF AVERAGE COMPUTATION TIME WITH VARIOUS STATE-OF-THE-ART METHODS (IN SECOND)

SAP Noise (in %)	FM [41]	CEF [42]	PWS [43]	AMEPR [44]	BDND [45]	CM [46]	SATV [47]	IAF [12]	DAMF [48]	AT2FF [28]		Proposed Approach
										DMSV	DMDV	
20	2.31	18.59	26.48	3957.94	219.36	12.58	23.96	12.04	1.23	2.43	2.44	2.40
50	2.31	18.59	26.48	3957.94	219.36	12.58	23.96	12.04	2.20	10.18	10.20	6.87
80	2.31	37.09	34.63	6486.45	220.47	17.02	28.78	26.32	3.50	31.70	31.72	12.70

than or equal to the critical difference (CD). For given value of α and degrees of freedom, the CD is defined as

where critical value q_α found in Table 5(b) in [50]. As discussed, two major statistical test i.e. Friedman test and BD test are performed for the statistical analysis. The first analysis is used to compare the various filtering methods by categorizing into ten different categories on the basis of PSNR values: FM, CEF, PWS, AMEPR, PB, BDND, CM, SATV, IAF, and proposed filtering method as shown in Table II.

Performing the Friedman test using the first analysis where $M = 15$ and $l = 10$.

$$\chi^2 = \frac{12 \times 15}{10 \times 11} \left[8.33^2 + 8.73^2 + 9.47^2 + 5.53^2 + 6.67^2 + 4.2^2 + 4.67^2 + 2.33^2 + 4^2 + 1.2^2 - \frac{10 \times 11^2}{4} \right] = 114.82$$

$$F_F = \frac{14 \times 116.92}{15 \times 9 - 116.92} = 79.66$$

The critical value of F_F (9, 126) statistic for $\alpha = 0.1$ is 1.68. Therefore, Null Hypothesis can be rejected at $\alpha = 0.1$.

As the Null Hypothesis is rejected, the corresponding CD between average ranks is computed using second analysis i.e. BD test as.

$$CD = q_\alpha \sqrt{\frac{l(l+1)}{6N}} \quad (21)$$

For, $l = 10$, $q_{0.1} = 2.539$

$$CD_{0.1} = 2.539 \times \sqrt{\frac{10 \times 11}{6 \times 15}} = 2.80$$

The Bonferroni–Dunn tests demonstrate that proposed filter is statistically better than FM, CEF, PWS, AMEPR, PB, BDND, CM, SATV with $\alpha = 0.1$, however, there is no consistent evidence to indicate the statistical differences from IAF.

The second statistical analysis is also performed to compare the performance of proposed filter with AT2FF [28]. In the AT2FF the UMF and LMF are also drawn using the primary MF but they are dependent on the window size (H). Table I presents the performance values of each of approaches at various datasets with different noise level. On the basis of performance values the Table III represents the rank of each approaches. Further, performing the Friedman test for the first analysis where, $M = 15$ and $l = 3$.

$$\chi^2 = \frac{12 \times 15}{3 \times 4} \left[2.53^2 + 2.47^2 + 1 - \frac{3 \times 4^2}{4} \right] = 22.53$$

$$F_F = \frac{14 \times 22.53}{15 \times 2 - 22.53} = 42.22$$

The critical value of F_F (2, 28) statistic for $\alpha = 0.1$ is 2.50. Therefore, the Null Hypothesis can be rejected at $\alpha = 0.1$. As the Null Hypothesis is rejected, CD between average ranks is computed using the second analysis i.e. BD test as.

For, $l = 3$, $q_{0.1} = 1.960$

$$CD_{0.1} = 1.960 \times \sqrt{\frac{3 \times 4}{6 \times 15}} = 0.72$$

The difference in average ranks of the proposed approach with AT2FF (i.e. DMSV* and DMSV**) are 1.53, and 1.47 respectively as given in Table III. The values of these difference are greater than CD at $\alpha = 0.1$. Therefore, it can be clearly ascertained that the proposed filter is also statistically better as compared to AT2FF.

B. Computation Complexity

For the comparative analysis experimentation was performed on desktop with *i7* processor and 8 GB RAM. The computation time of the proposed approach is little higher in compared to FM and DAMF, whereas it is less for rest of state-of-the-art filtering techniques as given in Table IV. The computation-time of the proposed approach is reduced because UMF and LMF are designed using exclusively two membership functions for any filter window size (H). Whereas, in the AT2FF the UMF and LMF are also drawn using the primary MF but these primary membership are dependent on the window size (H). Due to the window size dependent AT2FF filter takes large time to decide the threshold. The computation time of both the approaches are increased at higher noise due to increase in window size with better PSNR irrespective of noise level. But the computation time of AT2FF is larger in comparison of proposed approach because when the window size is increases at higher noise level the number of primary MFs are increase whereas in the proposed approach only two MFs are required to decide the threshold.

V. CONCLUSIONS

This paper presents a novel two-stage fuzzy filter for filtering SAP from digital images. In the first stage, adaptive threshold is designed to detect the noisy pixel by exclusively two different membership functions in a filter window. The detected pixel is denoised in the second stage using modified ordinary fuzzy logic in the respective window. The proposed filter is validated and compared with various state-of-the-art filtering techniques on several standard grayscale images at various noise levels. The comparative results shows that the robustness of the proposed filter is better quantitatively in terms of PSNR and qualitatively in terms of different SAP noise level. Additionally, filter is also able to preserve the desired image characteristics at a higher noise as shown in

Fig. 9f. The improvement in the performance is confirmed both visually and numerically. The statistical test is also performed which supports that the proposed filter is statistically better in comparison of various state-of-the-art methods.

REFERENCES

- [1] I. Pitas and A. Venetsanopou, "Nonlinear Digital Filters: Principles and Application," *Norwell, MA: Kluwer*, 1990.
- [2] J. Astola and P. Kuosmanen, "Fundamentals of Nonlinear Digital Filtering," *Boca Raton, FL: CRC*, 1997.
- [3] D. Brownrigg, "The weighted median filter," *Commun. Assoc. Computer*, pp. 807-818, 1984.
- [4] S. J. Ko and Y. H. Lee, "Center weighted median filters and their applications to image enhancement," *IEEE Trans. Circuits Syst.*, 38(9), pp. 984-993, 1991.
- [5] P. Zhang and F. Li, "A new adaptive weighted mean filter for removing salt-and-pepper noise," *IEEE Signal Process. Lett.*, 21(10), pp. 1280-1283, 2014.
- [6] C. L. P. Chen, L. Liu, L. Chen, Y. Y. Tang and Y. Zhou, "Weighted couple sparse representation with classified regularization for impulse noise removal," *IEEE Trans. Image Process.*, 24 (11), pp. 4014-4026, 2015.
- [7] L. Liu, *et al.*, "Mixed noise removal via robust constrained sparse representation," *IEEE Transactions on Circuits and Systems for Video Technology*, 28(9), pp.2177-2189, 2017.
- [8] L. Lu, W. Jin, and X. Wang, "Non-local means image denoising with a soft threshold," *IEEE Signal Process. Lett.*, 22(7), pp. 833-837, 2015.
- [9] A. Roy and R. H. Laskar, "Multiclass SVM based adaptive filter for removal of highdensity impulse noise from color images," *Appl. Soft Comput.*, vol. 46 , pp. 816-826, 2016.
- [10] C. S. Lee, Y. H. Kuo, and P. T. Yu, "Weighted fuzzy mean filters for image processing," *IFuzzy Sets Syst.*, 89(2), pp. 157-180, 1997.
- [11] C. S. Lee and Y. H. Kuo, "Adaptive fuzzy filter and its application to image enhancement," *IFuzzy Techniques in Image Processing*, Physica Verlag HD, pp. 172-193, 2000.
- [12] F. Ahmed and S. Das, "Removal of high-density salt-and-pepper noise in images with an iterative adaptive fuzzy filter using alpha-trimmed mean," *IEEE Trans. Fuzzy Syst.*, 22(5), pp. 1352-1358, 2014.
- [13] K. K. V. Toh and N. A. M. Isa, "Noise adaptive fuzzy switching median filter for salt-and-pepper noise reduction," *IEEE Signal Process. Lett.*, 17(3), pp. 281-284, 2010.
- [14] T. Mlange, M. Nachtegael, and E. E. Kerre, "Fuzzy random impulse noise removal from color image sequences," *IEEE Trans. Image Process.*, 20(4), pp. 959-970, 2011.
- [15] T. Schuster and P. Sussner, "An adaptive image filter based on the fuzzy transform for impulse noise reduction," *Soft Comput.*, vol. 21, pp. 3659-3672, 2017.
- [16] Y. Wang, J. Wang, X. Song, and L. Han, "An efficient adaptive fuzzy switching weighted mean filter for salt-and-pepper noise removal," *IEEE Signal Process. Lett.*, 23(11), 1582-1586, 2016.
- [17] M. G. Hidalgo, S. Massanet, A. Mir, and D. R. Aguilera, "Improving salt and pepper noise removal using a fuzzy mathematical morphology-based filter," *Appl. Soft Comput.*, vol. 63, pp. 167-180, 2018.
- [18] A. Roy, L. Manam and R. H. Laskar, "Region adaptive fuzzy filter: an approach for removal of random-valued impulse noise," *IEEE Transactions on Industrial Electronics*, 65(9), pp.7268-7278, 2018.
- [19] V. Singh, Harshvardhan, N. K. Verma and Y. Cui, "Optimal Feature Selection using Fuzzy Combination of Feature Subset for Transcriptome Data," *In 2018 IEEE International Conference on Fuzzy Systems (FUZZ-IEEE)*, pp. 1-8, 2018.
- [20] L. A. Zadeh, "The concept of a linguistic variable and its application to approximate reasoning-1," *Inform. Sci.*, vol. 8, pp. 199-249, 1975.
- [21] J. M. Mendel, and R. B. John, "Type-2 fuzzy sets made simple," *IEEE Trans. Fuzzy Syst.*, 10(2), pp. 117-127, 2002.
- [22] H. Bharadhwaj, V. Singh, and N. K. Verma, "A Type-2 Fuzzy Systems approach for Clustering based identification of a T-S Regression model," *In Computational Intelligence: Theories, Applications and Future Directions*, Vol. I, Springer, Singapore, pp. 359-374, 2019.
- [23] Q. Liang and J. M. Mendel, "Equalization of nonlinear time-varying channels using type-2 fuzzy adaptive filters," *IEEE Trans. Fuzzy Syst.*, 8(5), pp. 551-563, 2000.
- [24] A. Ba and M. E. Yksel, "Impulse noise removal from digital images by a detail-preserving filter based on type-2 fuzzy logic," *IEEE Trans. Fuzzy Syst.*, 16(4), pp. 920-928, 2008.
- [25] M. A. Khanesar, E. Kayacan, M. Teshnehlab and O. Kaynak, "Analysis of the noise reduction property of type-2 fuzzy logic systems using a novel type-2 membership function," *IEEE Trans. Syst., Man, and Cyb.*, 41(5), pp. 1395-1406, 2011.
- [26] M. E. Yuksel and A. Basturk, "Application of type-2 fuzzy logic filtering to reduce noise in color images," *IEEE CIM*, 7(3), pp. 25-35, 2012.
- [27] D. Zhai, M. Hao, and J. Mendel "Universal image noise removal filter based on type-2 fuzzy logic system and QPSO," *Int. Journal of Uncertainty, Fuzziness and Knowledge Based Syst.*, 20(2), pp. 207-232, 2012.
- [28] V. Singh, R. Dev, N. K. Dhar, P. Agrawal and N. K. Verma, "Adaptive Type-2 Fuzzy Approach for Filtering Salt and Pepper Noise in Grayscale Images," *IEEE Trans. Fuzzy Syst.*, 26(5), pp. 3170-3176, 2018.
- [29] P. Melin and O. Castillo, "Type-1 fuzzy logic. In Hybrid Intelligent Systems for Pattern Recognition Using Soft Computing," *Springer Berlin Heidelberg*, pp. 7-32, 2005.
- [30] L. A. Zadeh, "Fuzzy sets," *Info. and control*, 8(3), pp. 338-353, 1965.
- [31] R. K. Sevakula, and N. K. Verma, "Compounding General Purpose Membership Functions for Fuzzy Support Vector Machine Under Noisy Environment," *IEEE Trans. Fuzzy Syst.*, 25(6), pp.1446-1459, 2017.
- [32] N. K. Verma and M. Hanmandlu, "From Gaussian mixture model to non-additive fuzzy systems," *IEEE Trans. Fuzzy Syst.*, 15(5), pp. 809-827, 2007.
- [33] N. K. Verma and M. Hanmandlu, "Additive and Non-Additive Fuzzy Hidden Markov Models," *IEEE Trans. Fuzzy Syst.*, 18(1), pp. 40-56, 2010.
- [34] N. K. Verma, V. Singh, S. Rajurkar and M. Aqib, "Fuzzy Inference Network with Mamdani Fuzzy Inference System", *In Computational Intelligence: Theories, Applications and Future Directions*, Springer, Singapore, Vol. I, pp. 359-374, 2019.
- [35] S. Rajurkar, and N. K. Verma, "Developing deep fuzzy network with Takagi Sugeno fuzzy inference system," *In Fuzzy Systems (FUZZ-IEEE)*, pp. 1-6. IEEE, 2017.
- [36] N. N. Karnik, J. M. Mendel and Q. Liang, "Type-2 fuzzy logic systems," *IEEE Trans. Fuzzy Syst.*, 7(6), pp. 643-658, 1999.
- [37] D. J. Dubois, "Fuzzy sets and systems: theory and applications," *Academic press*, vol. 144, 1980.
- [38] V. Singh, N. K. Verma, and Y. Cui, "Type-2 Fuzzy PCA Approach in Extracting Salient Features for Molecular Cancer Diagnostics and Prognostics," *IEEE Transactions on Nanobioscience*, 2019.
- [39] Z. Wang, A. C. Bovik, H. R. Sheikh, and E. P. Simoncelli, "Image quality assessment: from error visibility to structural similarity," *IEEE Trans. Image Process.*, 13(4), pp. 600-612, 2004.
- [40] A. G. Weber, "The USC-SIPI image database version 5," *USC SIPI Report* 315, pp. 1-24, 1997.
- [41] K. S. Srinivasan and D. Ebenezer, "A new fast and efficient decision-based algorithm for removal of high density impulse noises," *IEEE Signal Process. Lett.*, 14(3), pp. 189-192, 2007.
- [42] U. Ghanekar, A. K. Singh, and R. Pandey, "A contrast enhancement-based filter for removal of random valued impulse noise," *IEEE Signal Process. Lett.*, 17(1), pp. 47-50, 2010.
- [43] V. Crnojevi, and N. Petrovi, "Impulse noise filtering using robust pixel wise S-estimate of variance," *EURASIP journal on Advances in Signal Process.*, 2010(8), 2010.
- [44] R. H. Chan, C. W. Ho, and M. Nikolova, "Salt and pepper noise removal by median type noise detectors and detail preserving regularization," *IEEE Trans. Image Process.*, 14(10), pp. 1479-1485, 2005.
- [45] P. E. Ng and K. K. Ma, "A switching median filter with boundary discriminative noise detection for extremely corrupted images," *IEEE Trans. Image Process.*, 15(6), pp. 1506-1516, 2006.
- [46] Z. Zhou, "Cognition and removal of impulse noise with uncertainty," *IEEE Trans. Image Process.*, 21(7), pp. 3157-3167, 2012.
- [47] R. Rojas and P. Rodriguez, "Spatially adaptive total variation image denoising under salt and pepper noise," *Proc. the Eur. Signal Process. Conf., Barcelona, Spain*, pp. 278-282, 2011.
- [48] U. Erkan, L. Gkrem, and S. Enginolu, "Different applied median filter in salt and pepper noise," *Computers & Electrical Engineering*, 70, pp. 789-798, 2018.
- [49] J. Sheskin, "Handbook of parametric and nonparametric statistical procedures", *CRC Press*, 2003.
- [50] J. Demsar, "Statistical comparisons of classifiers over multiple data sets", *The Journal of Machine Learning Research*, vol. 7, pp. 130, 2006.